Table 1 Fuzzy logic rule base

	X_2^{est}				
X_4^{est}	Negative	Negative small	Zero	Positive small	Positive
Positive	Very small	Small	Medium	Small	Very small
Positive small	Very small	Medium	Large	Medium	Very small
Zero	Medium	Large	Extra large	Large	Medium
Negative small	Very small	Medium	Large	Medium	Very small
Negative	Very small	Small	Medium	Small	Very small

been successfully employed, for example, using

$$R = 1, \qquad Q = 100I, \qquad \Theta = 1, \qquad \Xi = I \tag{8}$$

a single reduced controller, designed around the maximal dynamic pressure point, stabilizes all 24 points of the full-order model. Figure 2 presents representative results with a sixth-order controller.

IV. Fuzzy Logic Control

A fuzzy logic controller for the design point of maximum dynamic pressure was designed. Let the control u be of the form

$$u = -K_3 \cdot \dot{x}_{10}, \qquad \dot{\boldsymbol{x}}_9 = \boldsymbol{x}_{10}$$
$$\dot{x}_{10} = K_1 \cdot (\hat{x}_4 - \boldsymbol{x}_{10}) \cdot (K_{\text{fuzz}})^{K_4} + K_2 \cdot (\hat{\boldsymbol{x}}_2 - \boldsymbol{x}_9) \cdot K_{\text{fuzz}} \tag{9}$$

where x_9 and x_{10} are the controller states; $K_1 = 40.375$, $K_2 = 2697.9$, $K_3 = 2300$, and $K_4 = 0.85$ are constant parameters determined by the tuning process; K_{fuzz} is a time-variable gain determined by a fuzzy logic control algorithm; and $\hat{\boldsymbol{x}}_2$ and $\hat{\boldsymbol{x}}_4$ are the estimates of the state variables $\boldsymbol{x}_2$ and $\boldsymbol{x}_4$, respectively.

The fuzzy controller is implemented as a 25-rule Mamdani fuzzy system with two inputs and one output (see Table 1). The two inputs are the estimates of the state variables $\boldsymbol{x}_2$ and $\boldsymbol{x}_4$ and the output is K_{fuzz}.

Five membership functions are used to describe each of the inputs, namely, positive, small positive, zero, small negative, and negative. K_{fuzz} is represented by very small, small, medium, large, and extra large. The respective membership functions for the input/output parameters are obtained after a tuning process.

The fuzzy adaptation strategy is based on rules of the form IF/THEN that convert inputs to a single output, that is, conversion of one fuzzy set into another. The design is based on previous experience,[8] whereby large values of the inputs require a lightly damped system. However, when the plant state is in the vicinity of the desired state, the damping gain is large.

For aggregation we employ the bounded sum method, and for defuzzification we use the center-of-area scheme. The values of $\boldsymbol{x}_2$ and $\boldsymbol{x}_4$ are estimated using a full-order Luenberger observer based on the measurement $\boldsymbol{y}$. The closed-loop response for all 24 design points, using a single controller, was stable. Figure 3 presents represenative results.

V. Conclusions

NASA Langley Research Center's benchmark model was employed for the development and evaluation of three types of controllers for flutter supression. Of the two linear controllers, the full-order is superior in performance, but requires significanly higher amount of control effort. The fuzzy logic controller performance resembles those of the reduced-order linear controller.

Acknowledgment

The authors thank the reviewer for the great effort invested during the reviewing process and the enlightening comments and suggestions for improvement.

References

[1]Mukhopadhyay, V., "Transonic Flutter Suppression Control Law Design and Wind Tunnel Test Results," *Journal of Guidance, Control, and Dynamics*, Vol. 23, No. 5, 2000, pp. 930–937.

[2]Kelkar, A. G., and Joshi, S. M., "Passivity-Based Robust Control with Application to BACT Wing," *Journal of Guidance, Control, and Dynamics*, Vol. 23, No. 5, 2000, pp. 938–947.

[3]Waszak, M. R., "Robust Multivariable Flutter Suppression for BACT Wind-Tunnel Model," *Journal of Guidance, Control, and Dynamics*, Vol. 24, No. 1, 2001, pp. 147–153.

[4]Haley, P., and Soloway, D., "Generalized Predictive Control for Active Suppression," *Journal of Guidance, Control, and Dynamics*, Vol. 24, No. 1, 2001, pp. 154–159.

[5]Karpel, M., "Reduced-Order Models for Integrated Aerservoelastic Optimization," *Journal of Aircraft*, Vol. 36, No. 1, 1999, pp. 146–155.

[6]Zole, A., and Karpel, M., "Continuous Gust Response and Sensitivity Derivatives Using Space-State Models," *Journal of Aircraft*, Vol. 31, No. 5, 1994, pp. 1212–1214.

[7]Anderson, B. D. O., and Moore, J. B., *Optimal Control: Linear Quadratic Methods*, Prentice–Hall, Upper Saddle River, NJ, 1990, pp. 77–89.

[8]Cohen, K., Weller, T., and Ben-Asher, J., "Control of Linear Second-Order Systems by a Fuzzy Logic Based Algorithm," *Journal of Guidance, Control, and Dynamics*, Vol. 24, No. 3, 2001, pp. 494–501.

Optimal Trajectory Analysis for Deployment/Retrieval of Tethered Subsatellite Using Metric

Hironori A. Fujii* and Hirohisa Kojima†
Tokyo Metropolitan Institute of Technology, Tokyo 191-0065, Japan

I. Introduction

TETHERED subsatellite systems are attractive space structure components by which to construct large space structures because they are light in weight, packaged compactly, and sturdy in high tensile strength. The length of tether can be as long as 100 km in a scientific mission, which needs safe and smooth control for the deployment and retrieval of the tethered subsatellite.[1]

Fujii and Ishijima[2] have proposed a control algorithm to close the control loop stabilizing asymptotically the deployment and retrieval maneuver of the tethered subsatellite. Fujii and Anazawa[3] have also obtained an optimal path in the sense that the time integral of squared tension plus the squared in-plane angle is the performance index with inequality constraints on the control tension. Such optimal trajectories for the tethered subsatellite are studied in literatures[3,4] because they have much critical importance for control of such space systems.

The present Note is devoted to obtain an optimal trajectory in the geometric approach by connecting the initial position and final desirable position of the tethered subsatellite by the shortest length. The optimal index is clearly defined as the length of trajectories with sufficient physical meaning. The optimal path is a "straight line" measured by the Riemann metric because the orbiting tethered system is in the force fields of gravitation and orbital rotation. Minimizing the length of the trajectory of the subsatellite implies a process of finding a straight line to connect two positions, that is, a natural path for deployment/retrieval expected to be processed in minimum time and effort when only the length of tether is controlled.

The tethered subsatellite system is simplified in this analysis to a planer space pendulum, which consists of a particle and a tether without flexibility and is affected only by gravity-gradient torque. The present simple model is effectively employed to obtain a reference trajectory for any compensation control algorithm of a more

Received 7 June 2001; revision received 5 March 2002; accepted for publication 21 August 2002.

*Professor, Department of Aerospace Engineering, 6-6 Asahigaoka; fujii@tmit.ac.jp. Associate Fellow AIAA.

†Lecturer, Department of Aerospace Engineering, 6-6 Asahigaoka. Member AIAA.

complicated system with tether flexibility and out-of-plane motion.[4] The initial state of the tethered subsatellite is in vertical position with rotation zero, and its objective final state is also in vertical position having both the rotation and rotational velocity at zero. Deployment and retrieval procedures are thus described as closed trajectories connecting the origin of phase plane of the rotation of tether because the trajectories deviate from the origin in the Coriolis effect in maneuvering deployment/retrieval.

Optimal trajectories are obtained by numerical analysis in the cases of deployment and retrieval, and real time is transformed to a nondimensional time in the process of the analysis taking into consideration the constraint on the final real time.

The desired trajectory of minimum length is a straight line connecting the initial and final positions of the subsatellite if there is no dynamical environment affecting the system, but is different from the straight line because of the presence of the Coriolis force, which is the effect of rotational field on the deployment and retrieval of the tethered system. The optimal trajectories obtained for the deployment and retrieval process of the tethered subsatellite are shown to be symmetric to the vertical line because we are seeking a straight line, or the geodesic, which connects two dynamically equivalent states in the shortest path.

II. System Description

A model of the tethered subsatellite system treated in this Note is a gravity-gradient stabilized tethered subsatellite, as shown in Fig. 1. The subsatellite of mass m is assumed to be connected through a massless tether of length ℓ to a mother satellite, represented by the space shuttle in the figure. The center of mass of the mother ship C is assumed to follow a circular orbit with the angular velocity Ω affected only by the gravitation of the center of attraction O. Rotation of the tether in the orbital plane is denoted by θ in which only the planar motion in the orbital plane is considered.

The tethered subsatellite sets its equilibrium position along the line that connects the center of attraction towards the center of mass of the mother ship C, that is, along the X axis. This is because tether tension acts through the tether line and can only compensate for the difference between the orbital centrifugal force and the gravity of attraction along this line of equilibrium. The process of deployment or retrieval of the tethered subsatellite induces a velocity along the tether line, and the Coriolis effect naturally forces its position to deviate from the equilibrium line. Thus the process aims to alter an equilibrium position to another position with different length of the tether by controlling tether length. Deployment and retrieval control is recognized throughout in this Note as a process to place the position of the subsatellite from a state with $\ell(0)=\ell_0$, $\theta(0)=0$, and $\dot{\theta}(0)=0$ to another state also with $\ell(t_f)=\ell_f$, $\theta(t_f)=0$, and $\dot{\theta}(t_f)=0$. Dynamics of the present system is an effect of both of the rotating force field of the orbital motion and the gravitational force field caused by the center of attraction. The dynamics is nonlinear in the rotation and is also time varying nonlinear as a result of the time variation of the tether length.

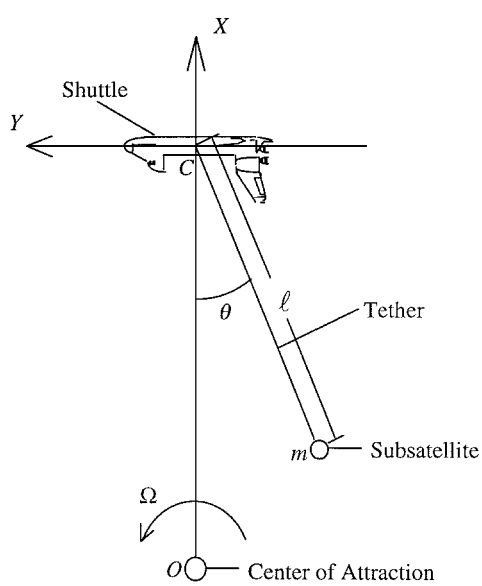

Fig. 1 Tethered subsatellite system.

III. Generated Dynamical System

Equations of motion of the subsatellite are written as follows:

$$\ddot{\ell} - \ell\dot{\theta}^2 - 2\ell\dot{\theta} - 3\ell\cos^2\theta = -(T/m\Omega^2) \tag{1a}$$

$$\ddot{\theta} + 2(\dot{\ell}/\ell)\dot{\theta} + 3\sin\theta\cos\theta + 2(\dot{\ell}/\ell) = 0 \tag{1b}$$

where T is the tension acting through the tether and the overdot denotes differentiation with respect to a normalized time $t^* = \Omega t$.

Let us consider only the equation of motion for rotation among Eqs. (1), and let the control variable be

$$u(t) := 2(\dot{\ell}/\ell) \tag{2}$$

then we are concerned only with the following equation of motion:

$$\ddot{q} + u\dot{q} + 3\sin q\cos q + u = 0 \tag{3}$$

where $q := \theta$ is used to denote the rotation. The preceding rotational motion depends on time t^* explicitly, and we define time t^* as a function of a new independent variable τ as follows:

$$\frac{\mathrm{d}t^*}{\mathrm{d}\tau} = \ell_0 \exp\left(\frac{1}{2}\int_0^{t^*} u\,\mathrm{d}t\right) = \ell(t^*) \tag{4}$$

Employing this transformation of the independent variable into Eq. (3), a new dynamical system is formed with the following function:

$$q'' + (\ell'/\ell)q' + 3\ell^2\sin q\cos q + 2\ell' = 0 \tag{5}$$

where the overdash denotes the differentiation with respect to τ.

IV. Trajectory Generator

In this Note the optimal trajectory is sought to minimize the following performance index J of the Riemann metric:

$$J = \frac{1}{2}\int_{t=0}^{t=t_f} (\dot{\ell}^2 + \ell^2\dot{\theta}^2)\,\mathrm{d}t = \frac{1}{2}\left[\int_{\tau=0}^{\tau=\tau_f}\left(\frac{\ell'^2}{\ell} + \ell q'^2\right)\mathrm{d}\tau\right] \tag{6}$$

with the nonholonomic constraints of equations of motion, Eq. (5).

The optimal index is clearly defined with sufficient physical meaning. The length of the trajectories in the orbital plane connecting the initial and final positions and the performance index, Eq. (6), denotes the real length of the trajectory in the orbital plane for the subsatellite to follow.

By defining p as $p = q'$ and considering Eqs. (5) and (6), Lagrangian L^* for the vakonomic mechanics is then obtained as follows:

$$L^* = \tfrac{1}{2}(\ell'^2/\ell + \ell q'^2) + \lambda_1(\tau)(q' - p)$$

$$+ \lambda_2(\tau)[p' + (\ell'/\ell)q' + 3\ell^2\sin q\cos q + 2\ell'] \tag{7}$$

where $\lambda_1(\tau)$ and $\lambda_2(\tau)$ are the Lagrange multipliers. Generalized momentum corresponding to the generalized coordinates q, p, and ℓ are defined as follows:

$$p_q := \frac{\partial L^*}{\partial q'} = \ell q' + \lambda_1 + \lambda_2\frac{\ell'}{\ell}, \qquad p_p := \frac{\partial L^*}{\partial p'} = \lambda_2$$

$$p_\ell := \frac{\partial L^*}{\partial \ell'} = \frac{\ell'}{\ell} + \lambda_2\frac{q'}{\ell} + 2 \tag{8}$$

with $\lambda_1 = p_q - \ell q' - \lambda_2(\ell'/\ell)$ and $\lambda_2 = p_p$. The corresponding Hamilton function is introduced as

$$H^* = p_q q' + p_p p' + p_\ell \ell' - L^* \tag{9}$$

and then, the optimal trajectory is generated through solving the two-point boundary-value problem governed by the following Hamilton equations:

$$q' \equiv \frac{\partial H^*}{\partial p_q} = p \tag{10a}$$

$$p' \equiv \frac{\partial H^*}{\partial p_p} = -p_\ell p - \frac{3}{2}\ell^2 \sin 2q + \frac{p_p}{\ell}p^2 - 2p_\ell + 4p_p p + 4p_p \ell \tag{10b}$$

$$\ell' \equiv \frac{\partial H^*}{\partial p_\ell} = -p_p p - 2p_p \ell + p_\ell \ell \tag{10c}$$

$$p'_q \equiv -\frac{\partial H^*}{\partial q} = 3p_p \ell^2 \cos 2q \tag{10d}$$

$$p'_p \equiv -\frac{\partial H^*}{\partial p} = p_\ell p_p - \frac{p_p^2}{\ell}p - 2p_p^2 + \ell p - p_q \tag{10e}$$

$$p'_\ell \equiv -\frac{\partial H^*}{\partial \ell} = 3p_p \ell \sin 2q + 2p_p p_\ell - 2p_p^2 - \frac{1}{2}p_\ell^2 + \frac{1}{2}p^2 + \frac{p_p^2 p^2}{2\ell^2} \tag{10f}$$

associated with the initial and final conditions for q, p, and ℓ.

The time response of tether length with respect to τ is obtained by solving numerically the preceding two-point boundary-value problem, and the final time t_f^* is specified by integrating Eq. (4) from 0 to τ_f with respect to τ. The final time of the new independent variable τ_f must be appropriately chosen in the present formulation if the constraint on the normalized time t_f^* is taken into consideration.

V. Numerical Analysis and Results

Geodesic is sought for a closed trajectory in the phase space (q, q'), which starts from the origin of the phase plane and returns to the origin satisfying the set of the ordinary differential equations, Eq. (10). The length of tether is treated in the nondimensional manner with respect to the final/initial length of the deployment/retrieval process and is controlled to deploy/retrieve from an initial length to a final objective length of 10 times/one-tenth of the initial length. The time period necessary to complete the deployment/retrieval process is set at one orbit. The closed trajectories are shown as the projection in the phase plane of tether rotation in Fig. 2. Trajectories of the tethered subsatellite by the present control of trajectory generation are shown in Fig. 3 in the orbital plane of X-Y coordinates, and trajectories are seen to be a smooth curve connecting the starting and the terminating points. We thus understand that the trajectory obtained in the present analysis is a straight line, or the geodesic, connecting the initial and the objective final positions in which both the rotation and its velocity are zero.

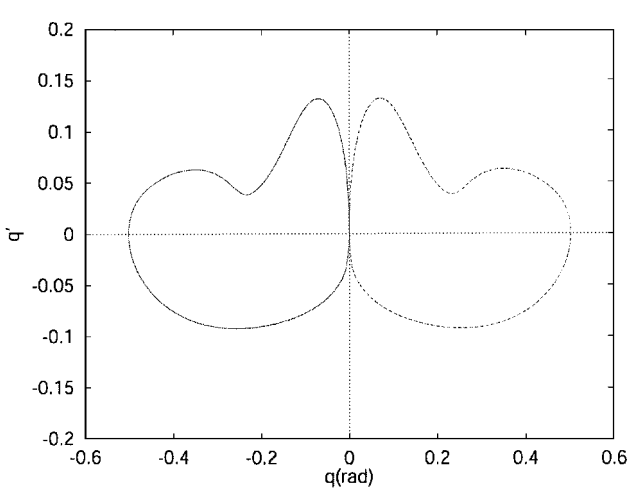

Fig. 2 Trajectories in the phase space of tether rotation: ——, deployment and – – –, retrieval.

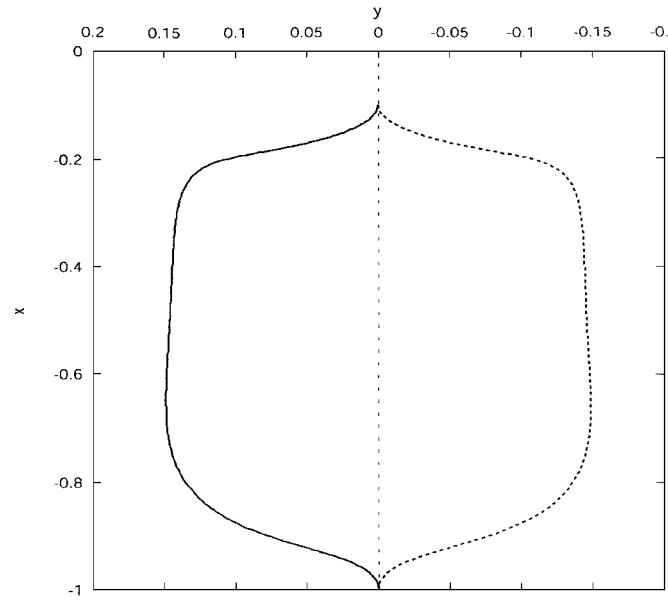

Fig. 3 Trajectories of the tethered subsatellite in the orbital plane: ——, deployment and – – –, retrieval.

Symmetry of trajectories for deployment and retrieval is clearly seen with respect to the vertical line in the orbital plane. The symmetry is understood to be natural because we are looking for a straight line connecting the initial vertical position and the objective final position in the effect of the rotational and gravitational field of orbital motion of the tethered satellite system employing a geometrical approach. The deployment and retrieval processes are only a natural manipulation of a dynamical system to transfer from an initial state to a final state where both states are along the vertical line.

VI. Conclusions

The optimal trajectory has been studied for the deployment and retrieval of a tethered subsatellite. The tethered subsatellite system is simplified to a space pendulum affected by gravity-gradient torque and librates in response to a command for a variation of length of the tether. The trajectory of the subsatellite is obtained by changing tether length for deployment and retrieval of the subsatellite while the tethered subsatellite is initially on the vertical line and then is recurring to the objective final state on the vertical line but different in the length of tether. The performance index of the optimal problem is selected as the Riemann metric to measure the length of trajectory of the subsatellite in the orbital plane.

The optimal trajectories have been obtained numerically by solving the two-point boundary-value problem for deployment and retrieval. Symmetry of the trajectories in deployment and retrieval process is naturally shown from the present approach of the geometrical method.

References

[1]Misra, A. K., and Modi, V. J., "Dynamics and Control of Tether Connected Two-Body Systems—A Brief Review," *Space 2000*, edited by L. G. Napolitano, AIAA, New York, 1983, pp. 473–514.

[2]Fujii, H., and Ishijima, S., "Mission Function Control for Deployment and Retrieval of a Subsatellite," *Journal of Guidance, Control, and Dynamics*, Vol. 12, No. 2, 1989, pp. 243–247.

[3]Fujii, H. A., and Anazawa, S., "Deployment/Retrieval Control of Tethered Subsatellite Through an Optimal Path," *Journal of Guidance, Control, and Dynamics*, Vol. 17, No. 6, 1994, pp. 1292–1298.

[4]Netzer, E., and Kane, T. R., "Deployment and Retrieval Optimization of a Tethered Satellite System," *Journal of Guidance, Control, and Dynamics*, Vol. 16, No. 6, 1993, pp. 1085–1091.